A&A manuscript no.
(will be inserted by hand later)

Your thesaurus codes are:
03(11.05.1, 11.11.1, 11.01.1, 11.06.1, 11.09.1 NGC 4816, 11.09.1 IC 4051)

ASTRONOMY
AND
ASTROPHYSICS
13.11.2008

The kinematically peculiar cores of the Coma cluster early – type galaxies NGC 4816 and IC 4051

D. Mehlert[1,⋆,⋆⋆], **R.P. Saglia**[1], **R. Bender**[1], **G. Wegner**[2]

[1] Universitätssternwarte München, D-81679 München, Germany
[2] Department of Physics and Astronomy, 6127 Wilder Laboratory, Dartmouth College, Hanover, NH 03755-3528, USA

accepted to be published in A&A, main journal

Abstract. The Coma cluster is one of the richest known cluster of galaxies, spanning about 4 dex in density. Hence it is the ideal place to study the structure of galaxies as a function of environmental density in order to constrain the theories of galaxy formation and evolution. For a magnitude limited sample of 35 E and S0 galaxies we obtained long slit spectra to derive the rotation curves, the velocity dispersion profiles and the radial gradients of the Mg, Fe and Hβ line indices. Here we report on two early – type galaxies which turned out to host the largest kinematically peculiar cores yet found in "normal" early – type galaxies: NGC 4816 hosts a decoupled counter rotating core with a radial extension along the major axis of 2.7 kpc, while IC 4051 has a co-rotating peculiar core with a sizes of 3.4 kpc. We combine our data with HST photometry and show that both cores are flattened central stellar disks which contribute less than 1 % to the total V band light of the galaxies, but are nevertheless conspicuous (1 – 2 $\times$ 10^9 $L_\odot$). The metallicity of the cores is 0.25 dex super solar and drops to solar and sub solar in the outer part of NGC 4816 and IC 4051, respectively. The mean stellar population in both central disks is old (8 – 12 Gyr) and highly overabundant in Mg_b relative to <Fe> ($\approx$ 0.5 dex). We discuss the evidence that these central disks formed via dissipational major merger events.

Key words: galaxies: elliptical and lenticular, cD – kinematics and dynamics – abundances – formations – individual: NGC 4816 – IC4051

Send offprint requests to: D. Mehlert (email: mehlert@usm.uni-muenchen.de)

⋆ Visiting astronomer at the German-Spanish Astronomical Center, Calar Alto, operated by the Max-Planck-Institut für Astronomie, Heidelberg jointly with the Spanish National Commission for Astronomy.

⋆⋆ Visiting astronomer at the Michigan - Dartmouth - M.I.T. Observatory, Kitt Peak, Arizona, operated by a consortium of the University of Michigan, Dartmouth College and the Massachusetts Institute of Technology.

1. Introduction

Kinematically peculiar cores are generally understood as being fossil fingerprints of the merging - and thus formation - history of the host galaxies (Kormendy 1984, Franx & Illingworth 1988, Bender 1988, Jedrzejewski & Schechter 1988). They have mostly been explained by either accretion of small spheroidal satellites by larger ellipticals (Kormendy 1984, Balcells & Quinn 1990, Balcells 1991) or as the result of major merging events by star dominated systems (Schweizer 1990, Barnes 1992a, Bender & Surma 1992, Hernquist 1993, Heyl et al. 1994). Up to now kinematically decoupled cores with radial extensions between 0.2 - 2.7 kpc have been found in a number of elliptical galaxies - lying in the field and in groups as well as in clusters (Bender 1990; see Sect. 5 for a detailed list).

Most peculiar cores have been shown to be due to a rapidly spinning disk – like component which presumably formed dissipatively (Bender 1988, 1990, Franx & Illingworth 1988, Rix & White 1992, Surma & Bender 1995). As shown by Bender & Surma (1992) the high absorption line strengths of the decoupled regions further argue against accretion of compact small galaxies and suggest a scenario analogous to massive spiral – spiral mergers (see also Davies et al. 1993). In this model the pre-enriched gas in the two merging components lost its angular momentum, settled in the central region and underwent a strong star formation phase. Though spiral – spiral mergers may still form ellipticals today (Kormendy & Sanders 1992), it is unlikely that most decoupled cores formed recently. Their location in the Mg – σ diagram indicates that the corresponding ellipticals have ages similar to normal ellipticals. Recent HST images of kinematically decoupled cores (Carollo et al. 1997) show that 45 - 60 % of them are in fact stellar central disks and confirm the idea, that most of them indeed have formed by dissipational merging

processes.
Finally HST imaging by Jaffe et al. (1994), Lauer et al. (1995) & Faber et al. (1997) has shown that the most luminous, anisotropic, boxy galaxies possess surface profiles with shallow cores while low luminous, rotationally flattened, disky ellipticals have power-law profiles (confirming earlier claims by Nieto et al. 1991).

Here we present kinematical and line index profiles as well as HST surface brightness profiles for the two Coma galaxies IC 4051 and NGC 4816, which host the largest cores yet found in early – type galaxies.
In Sect. 2 we describe the spectroscopic observations, data reductions and the results of the kinematical analysis and line strength measurements. The photometric data obtained with the Hubble Space Telescope (HST) and the MDM 1.3 m telescope are described in Sect. 3, where we derive the surface brightness profiles and other photometric parameters. We summarize the combined spectroscopic and photometric results in Sect. 4. Finally we discuss formation scenarios for NGC 4816 and IC 4051 in Sect. 5.

2. Spectroscopy

2.1. Observations & data analysis

Long-slit spectra centered on the 5170 Å Mg triplet of NGC 4816 and IC 4051 were taken along their major axes. NGC 4816 was observed at the 3.5 m telescope of the German-Spanish Astronomical Center on Calar Alto (CA) in 1996 (see Table 1). IC 4051 was observed with the 2.4 m telescope of the Michigan-Dartmouth-M.I.T. (MDM) observatory on Kitt Peak in 1995. Additionally, during both runs we obtained spectra for ten K – Giant template stars, trailed and wiggled across the slit. The standard reduction (bias & dark subtraction, flat fielding, wavelength calibration, sky subtraction, correction for CCD misalignment) was carried out with the image processing package MIDAS provided by ESO.
After continuum subtraction and radial binning along the slit we achieved a S/N $\geq$ 40/Å for all of our data. We determined the line-of-sight-velocity-distributions (LOSVDs) by using the Fourier Correlation Quotient (FCQ) method (Bender 1990), which provides us with the stellar rotational velocities v_{rot}, the velocity dispersions σ and the first orders of asymmetric (H_3) and symmetric (H_4) deviations of the LOSVDs from real Gaussian profiles (van der Marel & Franx 1993 ; Bender et al. 1994). As expected, we find that the FCQ method is little influenced by template mismatching (Bender 1990). The "best" template star minimizing the asymmetric deviations (H_3) of the LOSDV from a real Gaussian profiles turned out to be HR 6817. Following Bender et al. (1994), Monte Carlo simulations were made to find the best fit-order for the continuum, to check for systematic effects and to estimate errors. For NGC 4816 two exposures with an atmospherical seeing of FWHM = 1.2" and one with FWHM = 3.7" were available. The latter one was excluded for the final analysis, but was used to check, whether the large slit width (3.6") affected the spectral resolution significantly for good seeing conditions. The three individual exposures did not produce significant differences within the errors.
Line strength indices were derived following Faber et al. (1985) and Worthey (1992) from flux calibrated spectra, rebinned radially as before. Furthermore, we corrected for velocity dispersion broadening and calibrated our measurements to the Lick system using stars from Faber et al. (1985). The errors are derived from photon statistics and CCD read-out noise.

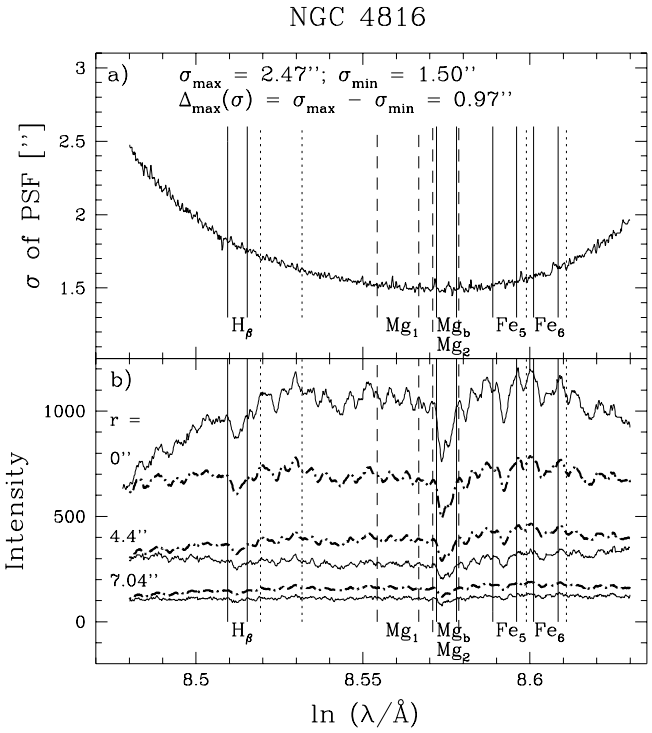

Fig. 1. (a) The measured Gauss width σ at each wavelength for one single frame of NGC 4816. We measured σ inside a radius of 7", which turned out to be the radius at which the focus variation starts to effect the continuum of the measured spectra. For H_β, Mg_b, Fe_5 and Fe_6 the line windows defined by Faber et al. (1985) are indicated (solid lines). For the Mg_1 and Mg_2 indices the line windows (long dashed lines) and the windows for their pseudo continuum (short dashed lines) are shown. **(b)** The spectra of NGC 4816 at different radii before (thin solid line) and after (fat dashed dotted line) the focus correction. The different continua shapes in the uncorrected spectra are evident. Like in Fig. **(a)** the windows for the measured indices are indicated.

The line index profiles for NGC 4816 needed further treatment. At small radii some of them show unreal features caused by the varying focus of the spectrograph in the

Galaxy	Telescope	Detector	$\lambda\lambda$ – range [Å]	Scaling ["/pix]	Slit width ["]	Resolution	Exp. time [s]	PA (N to E)	seeing (FWHM)
NGC 4816	CA 3.5 m	TI 1024 x 1024	4730 – 5700	0.89	3.6	1.17 Å 67.6 km/s	7000	78°	1.2"
IC 4051	MDM 2.4 m	TI 1024 x1024	4300 – 6540	0.77	1.7	2.3 Å 149.7 km/s	10800	106°	1.8"

Table 1. Setup of the observing runs

dispersion direction, which depends slightly on the wavelength. Following Gonzales (1993), this effect is only detectable if the variation of the focus' point spread function (PSF) is dominant compared to the atmospherical seeing (FWHM). For NGC 4816 the focus variation was the dominant effect and we developed a new method to correct for this "focus effect": For each single exposure of NGC 4816 we measured the central Gaussian width $\sigma(\lambda)$ of the radial profile at each wavelength (Fig. 1a) and noted that σ is larger at the blue and red end of the spectra compared to the central wavelength. Therefore blue and red light is spread more radially than light in the center of the spectrum. Consequently, the spectrum's continuum shape varies with radius (see Fig. 1b; thin solid line) and leads to unreal central features in the measured line index profiles. The Mg_1 and Mg_2 indices defined by Faber et al. (1985) are affected most, because their pseudo continua are $\approx$ 200 Å apart from the line windows. For all the other line indices the continuum and line windows are close to each other. H_β and the Fe indices are in the red and blue wing of the spectra and thus slightly affected, while the Mg_b index at the central wavelength is almost unaffected. To correct for this focus variation in the exposures of NGC 4816 we convolved all radial profiles with the wavelength depending width $\sigma_{broad} = (\sigma^2_{max} - \sigma^2(\lambda))^{1/2}$ (see Fig. 1a). As a result the radial profiles have the width $\sigma_{max} = 2.47$" at all wavelength. Furthermore, the continuum shapes of the spectra are the same for all radii (see Fig. 1b; fat dashed dotted line) and the artificial features in the line index gradients disappear (see Mehlert 1998 for a more detailed description). For the spectra of NGC 4816 the maximum broadening width is $\sigma^{broad}_{max} = (\sigma^2_{max} - \sigma^2_{min})^{1/2}$ =1.96" (σ_{min} =1.5"; see Fig. 1a). The resulting PSF for the measured line index profiles (shown in Fig. 2b) has $\sigma_{res} = ((\sigma^{broad}_{max})^2 + \sigma^2_{seeing})^{1/2} = 2.0$" and $FWHM_{res} = 4.7$" .
For IC 4051 no "focus correction" was necessary, because the atmospherical seeing was dominant during the observations.

2.2. Kinematical profiles and line index gradients

Figs. 2 and 3 show the kinematical profiles (a) together with the line indices (b) of NGC 4816 and IC 4051, respectively.

NGC 4816:
This galaxy contains a kinematically decoupled core, which is counter-rotating with respect to the main spheroid at a maximum velocity v_{max} = 30 km/s. The kinematical break radius is $r_b = 4$", which is 2.7 kpc in the Coma cluster (1' = 40 kpc; H_o = 50 km/s/Mpc). The velocity dispersion is σ_b = 220 km/s at r_b and its gradient gets much steeper inside the core, rising to a central value of $\sigma_o \approx$ 260 km/s. Finally, H_3 changes sign at the core radius. The central velocity dispersion measured by Davies et al. (1987) lies a bit above our profile, but still agrees with it within the errors.

For NGC 4816 the line indices measured with (large symbols) and without (small dots) the focus correction described in Sect. 2 are shown and the need and improvement for the Mg_2 index is obvious. Without focus correction the profile of the Mg_2 index is disturbed out to 7".
For the focus corrected profiles we find an increase of slope in the Mg_2 as well as in the Mg_b line profile inside 8", which is larger than r_b (see section 4 for explanation). Beyond 8" the Mg_b index is constant. The mean iron index <Fe> = (Fe_5 + Fe_6) / 2 and the combined index [MgFe] = (Mg_b <Fe>)$^{1/2}$ do also increase inside 8" and stay constant beyond that point. The H_β index shows a slight increase towards the outer parts of the galaxy, but is dropping at the very outer (less reliable) data point. The Mg_2 value derived by Davies et al. (1987) is a little larger than our data, but still agrees within the errors.

IC 4051:
This galaxy contains a peculiar core which is co-rotating with the main spheroid at a maximum projected velocity v_{max} = 60 km/s. The core's kinematics are detectable to a radius of 5 ", which is 3.4 kpc in the Coma cluster. It is *not clear* whether the core of IC 4051 is really *decoupled* from the rotation of the main body, since the velocity curve does not drop to exactly 0 at the break radius r_b. The velocity dispersion is σ_b = 220 km/s at r_b and its gradient gets much steeper inside the core, rising to a central value of $\sigma_o \approx$ 280 km/s. Note that the H_3 parameter is negative for the co-rotating core. Jørgensen et al. (1995) as well as Davies et al. (1987) measured the central velocity dispersion for this galaxy, deriving values in good agreement with ours.

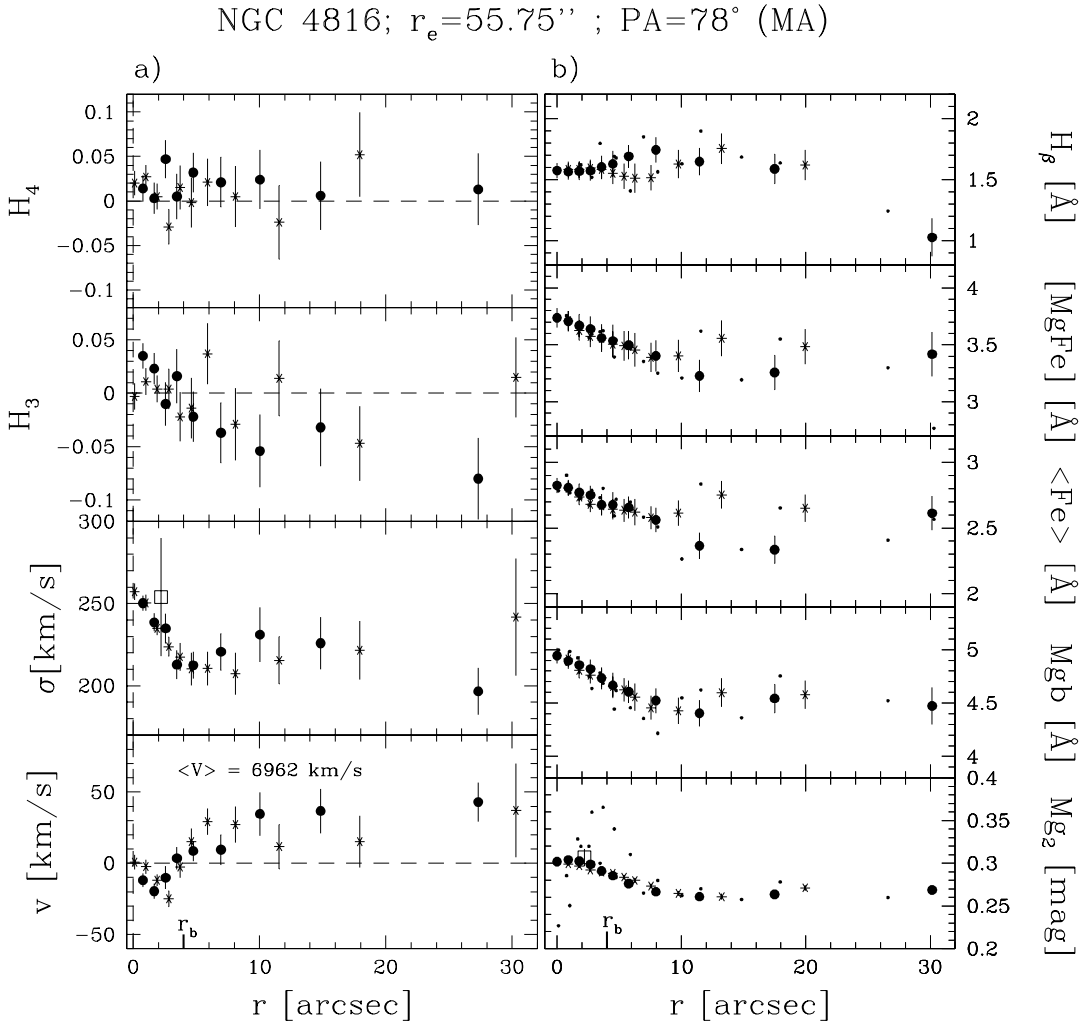

Fig. 2. (a) Kinematical parameters and measured line indices **(b)** for NGC 4816 along the major axis. The curves are folded around the nucleus of the galaxy and different symbols refer to different sides. For **(b)** the profiles before (small dots) and after focus correction (large symbols) are shown. Open squares are results from Davies et al. (1987) who used a 4"×4" aperture. We determined the equivalent radius along our used slit via $r_{d87} = 0.5 \times$ (4"×4"/ slitwidth). Panels from bottom to top: **(a)** (1) Rotation velocity v(r) relative to the system velocity, (2) velocity dispersion σ(r), (3-4) Gauss-Hermite moments H_3 and H_4. **(b)** (1-2) Mg_2 and Mg_b, (3) mean Fe index <Fe> = (Fe_5 + Fe_6)/2, (4) the combined index [MgFe] = (Mg_b <Fe>)$^{1/2}$, (5) H_β index.

The Mg_b index is unusually high, showing values up to 5.5 Å in the center of the galaxy. It is constant in the core region, but decreases strongly beyond r_b. The asymmetry of the Mg_b profile in the center of the galaxy as well as in the outer parts is probably due to contamination from [NI] emission lines in the interstellar medium (Goudfrooij & Emsellem 1996). [NI] emission can artificially increase the measured Mg_b index. The asymmetry itself arises from the fact that the stars and the gas may have different velocities up to 100 km/s (Bertola et al. 1995). Additionally, as shown by Goudfrooij & Emsellem (1996), the Mg_2 index is much less disturbed by the [NI] emission lines, because of its different continuum definition. However, the S/N and spectral resolution of our data are insufficient to quantify this effect. In this galaxy the mean Iron index <Fe> shows a steep increase towards the center starting at the break radius, while the combined index [MgFe] is constantly increasing towards the center of the galaxy. A steep decrease of the H_β absorption index is present outside 7". The inspection of the H_β absorption lines shows that they might be partially filled by emission like features outside this radius. As above, the S/N and resolution of

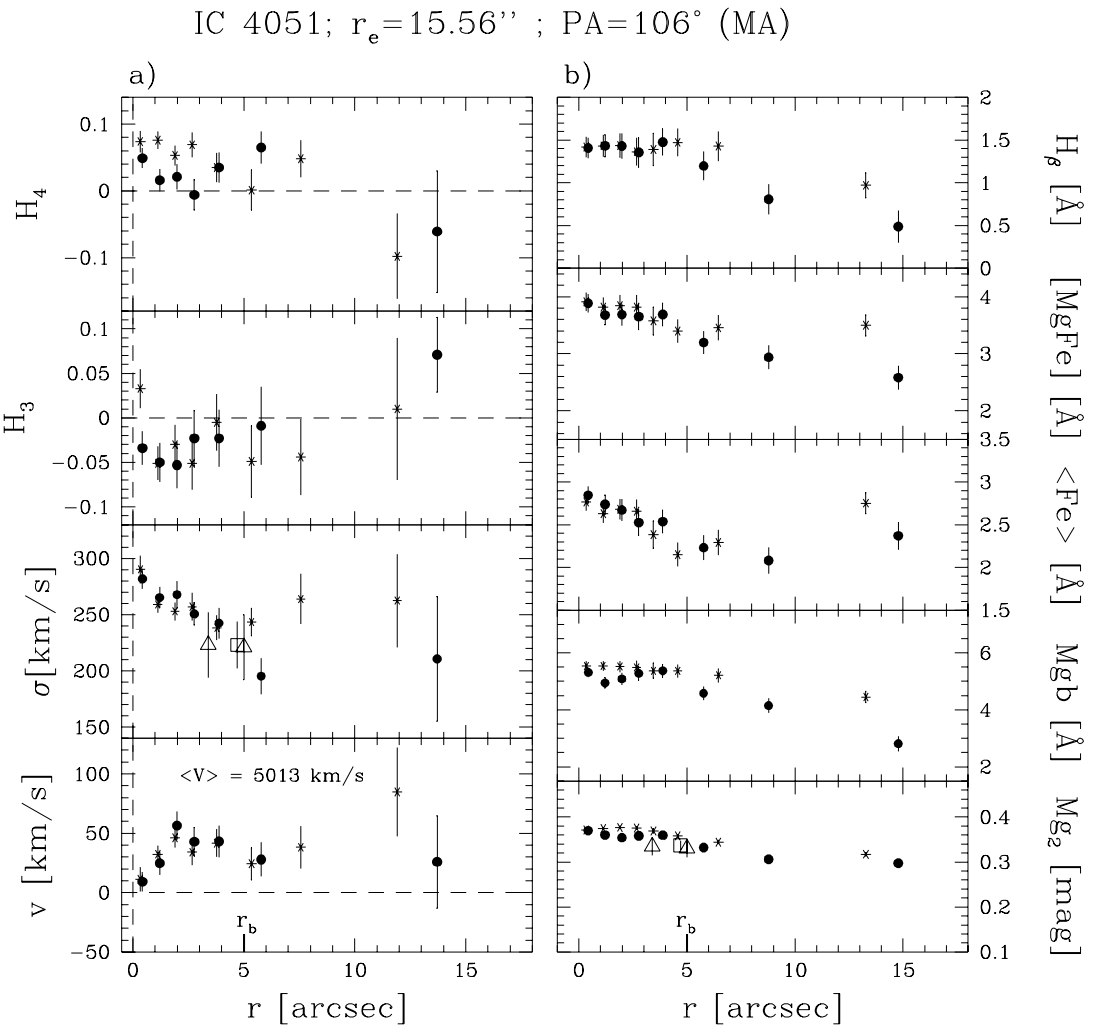

Fig. 3. Kinematical parameters **(a)** and measured line indices **(b)** for IC 4051 along the major axis. The curves are folded around the nucleus of the galaxy with different symbols referring to different sides. Open triangles represent data from Jørgensen et al. (1995) and open squares those from Davies et al. (1987). The latter used a 4"×4" aperture. We determined the equivalent radius along our used slit via $r_{d87} = 0.5 \times$ (4"×4"/ slitwidth). Panels from bottom to top: **(a)** (1) Rotation velocity v(r) relative to the system velocity, (2) velocity dispersion σ(r), (3-4) Gauss-Hermite moments H_3 and H_4. **(b)** (1-2) Mg_2 and Mg_b, (3) mean Fe index <Fe> = (Fe_5 + Fe_6)/2, (4) the combined index [MgFe] = (Mg_b <Fe>)$^{1/2}$, H_β index.

the data do not allow to quantify the effect. Central values of Mg_2 are provided again by Jørgensen et al. (1995) and Davies et al. (1987) and agree with our data.

3. Photometry

3.1. HST observations & data analysis

HST images were available for both galaxies, NGC 4816 (Principal Investigator: John Lucey; Proposal ID: 5997) and IC 4051 (Principal Investigator: James Westphal; Proposal ID: 6283). For NGC 4816 exposures with 800 s in total are available with the F606W Filter, while for IC 4051 eight full-orbit WFPC2 exposures (20500 s in total) with the F555W Filter (λ_c = 5957 Å) and two (5200 s in total) with F814W (λ_c = 7940 Å) were obtained. Cosmic ray elimination and the production of a median frame from multiple observations were carried out within "STSDAS" packages of the image processing system IRAF [1] (Tody 1993).

[1] IRAF is distributed by the National Optical Astronomy Observatories, which are operated by the Association of Uni-

The subsequent analysis was done within MIDAS using the data of the Planetary Camera (PC), which has a scaling of 0.04555"/pixel. The sky values were determined from the Wide Field Camera (WFC) images in areas which were at least 55" away from the galaxy's center. After sky subtraction the foreground stars and galaxies were either replaced with values from the opposite side of the galaxy or totally removed and excluded from the analysis. The photometric zero points were derived and converted to the Johnson-Cousins system following the procedure described in Holtzman et al. (1995). We added a constant shift of 0.115 mag to correct for infinite aperture and determined the I(F814W), V(F606W)and V(F555W) band zero points to be 21.67 mag, 23.33 mag and 22.57, respectively.

The deviations of the isophotes from ellipses were studied by means of Fourier series expansions (Bender & Möllenhoff, 1987). The resulting fourth cosine coefficients a_4 indicates boxy (negative values) or disky isophotes (positive values). Additionally, we estimated the brightness profile of the existing central disks with the decomposition method developed by Scorza & Bender (1995). The principal idea is to consider galaxies with a positive a_4 parameter to be a composition of an ideal elliptical bulge with $a_4 = 0$ and a thin disk. The model disk is described by an exponential intensity profile and parameterized by the scale length r_h, the central surface brightness I_0, the position angle P.A. and the inclination angle[2] i. These free parameters are varied in an iterative process until a bulge having perfectly elliptical isophotes ($a_4 \approx 0$) remains. We also determined the ratio of the disk's and bulge's luminosity (D/B = $L_D/(L_G$ - $L_D)$) for the whole galaxy and inside the kinematically detected break radius r_b. For the distance module of the Coma cluster we used $(m - M) = 35.7$ mag and the V and I absolute magnitude of the Sun are $M_{\odot,V} = 4.84$ mag and $M_{\odot,I} = 4.03$ mag.

For IC 4051 we also derived the V-I colour and its gradient. Since the PSF of the HST is different for the two filters and varies with the position on the CCD, we convolved each frame with the PSF[3] of the other filter. Finally we get the same resulting PSF for both frames.

The values of the total magnitude m_T, the surface brightness SB and the colour have been corrected for galactic extinction an K – corrected. We have used the B band galactic extinction determined by Burstein et al. (1987) for both NGC 4816 ($A_B = 0.03$ mag) and IC 4051 ($A_B = 0.05$ mag). For the filters we used, we assumed $A_\lambda = k_\lambda A_B$ and following Seaton (1979) we determined the values $k_V = 0.79$, $k_R = 0.58$ and $k_I = 0.48$. For the K – correction we used values provided by Rocca-Volmerange & Guiderdoni (1988) ($K_V = 0.041$ mag, $K_R = 0.028$ mag, $K_I = 0.0$ mag). Finally, we corrected the surface brightness for cosmological dimming.

versities for Research in Astronomy, Inc., under cooperative agreement with the National Science Foundation of the USA.

[2] where $i = 0°$ means face on, $i = 90°$ edge on.

[3] The PSFs where obtained with the TINYTIM routine.

3.2. MDM observations & data reduction

We also obtained Kron-Cousins R band CCD surface photometry for NGC 4816 at the 1.3 m telescope of the MDM observatory in March 1995. We used a Loral 2048 x 2048 chips with a scaling of 0.508" per pixel and observed NGC 4816 for 500s with a PSF of 2". Sky subtraction, cosmic ray elimination and the removal of foreground stars were performed with MIDAS packages. We carried out the same isophote analysis and surface brightness fit as for the HST data. The zero point was estimated by using V band aperture photometry from Burstein et al.(1987) and using a typical colour for elliptical galaxies V-R = 0.65 mag (Poulain & Nieto 1994). Total magnitudes m_T and half luminosity radii r_e were derived using the algorithm of Saglia et al. (1997a), which fits the surface brightness profiles as a sum of seeing convolved $r^{1/4}$ and exponential components.

3.3. Isophotal analysis and photometric profiles

NGC 4816:

Fig. 4a shows the surface brightness profiles as well as the results of the isophotal analysis for the HST V band. We appended the "colour shifted" MDM R band data in the outer part of the galaxy (> 20"). The best fit of the MDM surface brightness profile is given by a sum of an $r^{1/4}$ law and an exponential component and is also shown in the figure. Inside the kinematically detected break radius (4"), the surface brightness from the HST data shows the exponential profile typical for a disk. Additionally the a_4 parameter is positive inside the core region. Outside the core the amplitudes of a_4 parameter become slightly negative. The a_6 parameter is slightly negative inside the core, while the amplitudes for the other Fourier coefficients are small and the mean ellipticity $\epsilon = 0.2$. We also show the surface brightness profile of the best model disk from the decomposition. For the remaining bulge we plot the a_4 and a_6 parameter, the P.A. and ϵ in Fig. 4b together with the data values for the whole galaxy. The corrected photometric parameter for the central disk we determined from the HST data are presented in Table 2. Additionally m_T and r_e derived from the MDM data for the whole galaxy and those available from the literature are listed in Table 3. The discrepancy between the r_e we measured and the literature values is due to different maximal radial extension of the profiles. Our surface brightness profile extends to $\approx$ 170", while the profiles of Andreon et al. (1996, 1997), Lucey et al. (1991) and Burstein et al. (1987) only reach to $\approx$ 30", 50" and 40", respectively. Additionally only a pure $r^{1/4}$ profile was fitted, taking no account of a possible

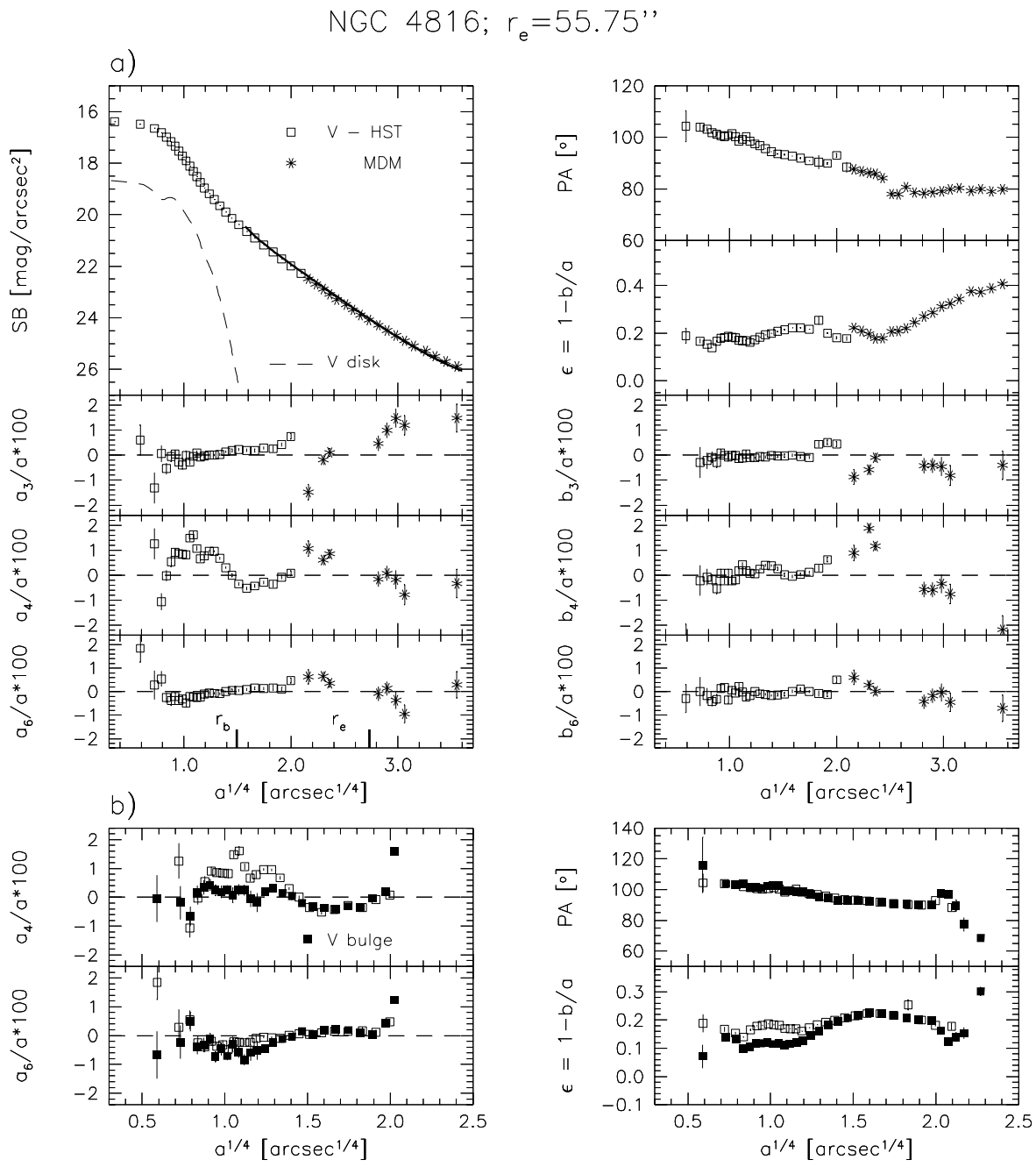

Fig. 4. (a) Results of the isophote analysis of NGC 4816 from the HST V band data (open symbols) are plotted versus the major axis a. "Colour shifted" MDM R band data are appended for the outer part of the galaxy (a > 20"). The best fit of the MDM surface brightness profile - a sum of an $r^{1/4}$ law and an exponential component - is overplotted (fat solid line). The fit is only shown in the outer region, since the groundbased MDM profile starts to deviate from the HST profile inside 6" due to different PSFs. Left panels (top to bottom): (1) Surface brightness profile SB of the whole galaxy and the central disk only (dashed line), (2-4) Fourier coefficients a_3/a, a_4/a, a_6/a. Right panels (top to bottom): (1) Position angle PA, (2) ellipticity ϵ, (3-5) Fourier coefficients b_3/a, b_4/a b_6/a. **(b)** Results of the decomposition for the HST data (open symbols - whole galaxy; filled symbols - bulge only) plotted versus the major axis a. Left panels (top to bottom):(1-2) Fourier coefficients a_4/a, a_6/a. Right panels (top to bottom): (1) Position angle PA, (2) ellipticity ϵ.

Galaxy	Filter	m_d [mag]	r_h ["]	i	PA_d	L_d [$10^9 L_\odot$]	$(D/B)_{tot}$	$D/B(r \leq r_b)$
NGC 4816	V	17.79	0.94	64°	100°	1.26	1.0 %	6.9 %
IC 4051	V	19.12	0.74	65°	90°	0.37	0.4 %	2.5 %
IC 4051	I	17.53	0.90	65°	90°	0.79	0.5 %	2.8 %

Table 2. Photometric parameters for the central disks of NGC 4816 and IC 4051

exponential component.

Galaxy	Filter	m_T [mag]	r_e ["]	Source
NGC 4816	R	11.61	55.75	this work
NGC 4816	R	11.62	27.54	Andreon et al. (1996)
NGC 4816	V	12.66	25.12	Andreon et al. (1997)
NGC 4816	V	12.90	17.14	Lucey et al. (1991)
NGC 4816	V	12.82	21.20	Burstein et al.(1987)
NGC 4816	B	13.79	21.20	Burstein et al.(1987)
IC 4051	R	12.46	15.56	Saglia et al. (1997b)
IC 4051	R	12.77	10.72	Andreon et al. (1996)
IC 4051	r	12.82	19.50	Jørgensen et al. (1992)
IC 4051	V	13.10	18.66	Lucey et al. (1991)
IC 4051	V	13.04	20.30	Burstein et al.(1987)
IC 4051	B	13.92	22.39	Jørgensen et al. (1992)
IC 4051	B	14.01	20.30	Burstein et al.(1987)

Table 3. Photometric parameters from literature (and own photometry) for NGC 4816 and IC 4051

IC 4051:
The surface brightness profiles and the results of the isophotal analysis are shown in Fig. 5a for both, the Johnson I and the V band exposure. We appended the "colour shifted" R band data from Saglia et al. (1997b) in the outer part of the galaxy (> 20"). The best fit of the R band surface brightness profile is given by a sum of an $r^{1/4}$ law and an exponentiell component and is also shown in the figure. In both the I and the V band the a_4 parameter is positive inside 5", which is the size of the co-rotating decoupled component, detected in the velocity curve. Additionally, the a_6 parameter is slightly negative inside the core, while the amplitudes for the other Fourier coefficients are small and the mean ellipticity $\epsilon = 0.2$. We also show the surface brightness profile of the best model disk from the decomposition. We plot the a_4 and a_6 parameter, the P.A. and ϵ for the remaining bulge in Fig. 5b together with the results for the whole galaxy. The corrected photometric parameter for the central disk we determined from the HST data are presented in Table 2 for both filters. Additionally, the total magnitude m_T and the effective radius r_e for the whole galaxies available from the literature are listed Table 3. The central colour $(V\text{-}I)_o$ is 1.355 mag and the V-I colour profile is show in Fig. 6. We derived a mean colour gradient $\Delta(V-I)/\Delta log(r)$ within 10" of -0.018 mag/dex by a linear fit. For comparison, Jørgensen et al. (1992) found a B-r gradient of -0.09 mag per dex in radius inside r_e.

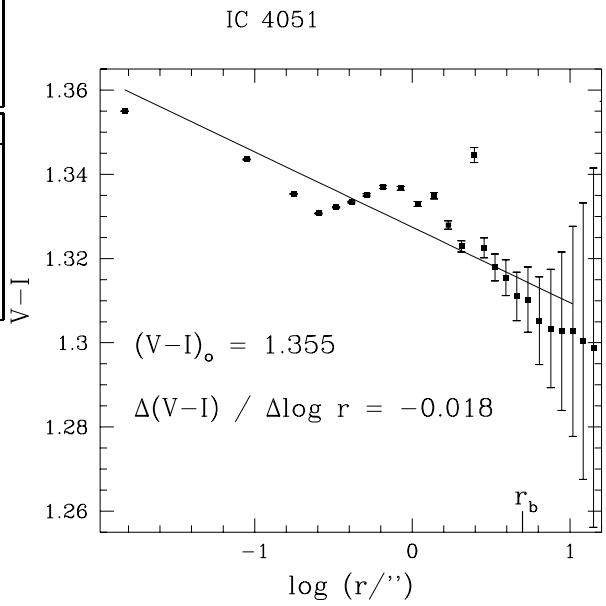

Fig. 6. V - I colour profile of IC 4051 and the results of the least square fit for the colour gradient within 10".

4. Results

The early – type galaxy **NGC 4816** hosts a *decoupled* counter rotating *core* with a size of $r_b = 4$" (Fig. 2a). Inside this core the H_3 parameter, which measures the asymmetric deviations from a gaussian velocity distribution, is slightly positive where $v < 0$. This confirms Bender et al. (1994), who find that H_3 becomes systematically negative with increasing $v/<\sigma>$. Hence, the LOSVD in the core of NGC 4816 are *intrinsically asymmetric*, showing an excess of fast rotating stars.
The isophotes inside 4" are clearly disky, which is derived

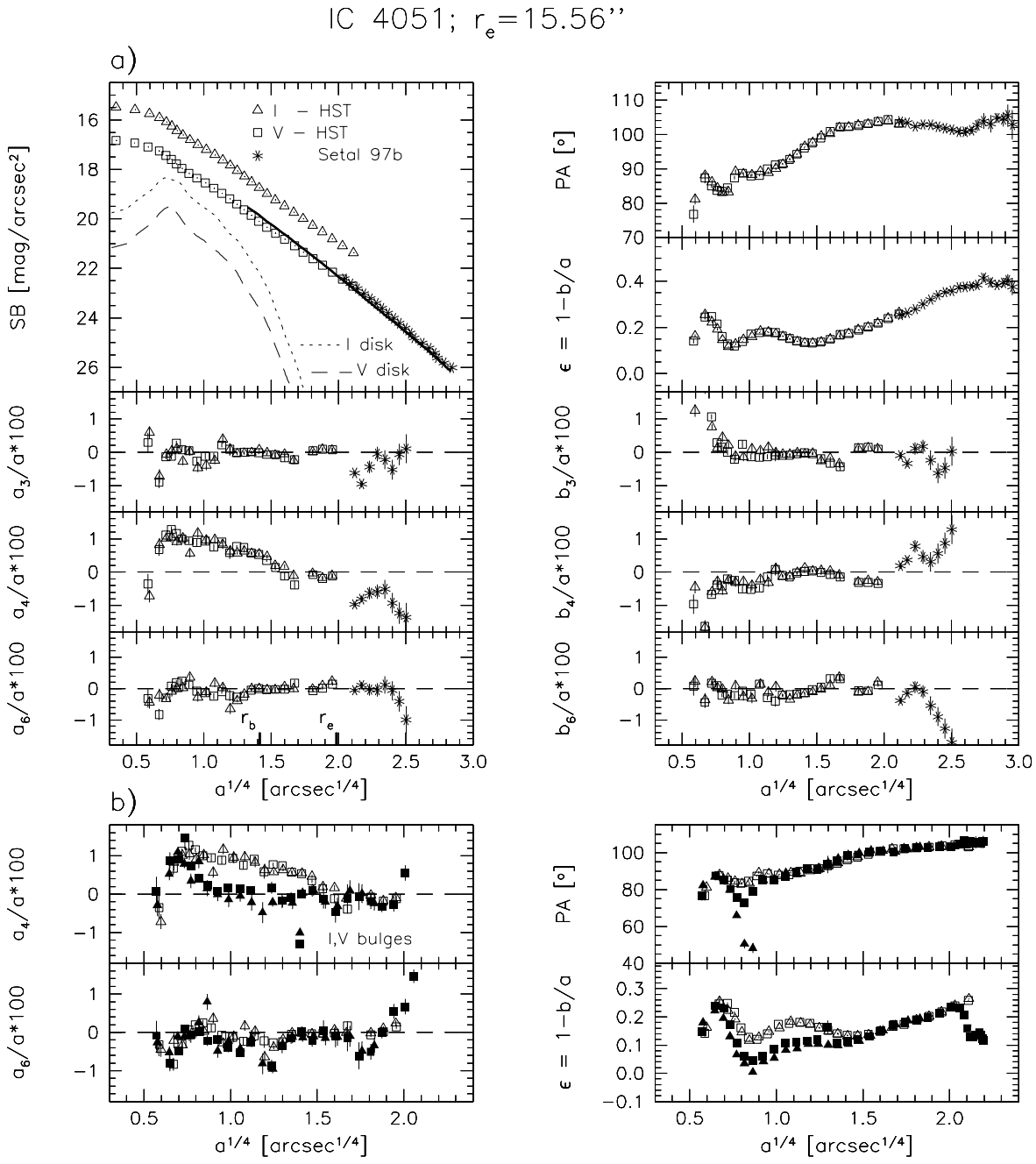

Fig. 5. (a) Results of the isophote analysis of IC 4051 from the HST V and I band data (open symbols) are plotted versus the major axis a. "Colour shifted" R band data from Saglia et al. (1997b) (stars) are appended for the outer part of the galaxy (a > 20"). The best fit of the R band surface brightness profile - a sum of an $r^{1/4}$ law and an exponential component - is overplotted (fat solid line). The fit is only shown in the outer region, since the groundbased R band profile starts to deviate from the HST profile inside 3" due to different PSFs. Left panels (top to bottom): (1) Surface brightness profile SB of the whole galaxy and the central disk only (short and long dashes), (2-4) Fourier coefficients a_3/a, a_4/a, a_6/a. Right panels (top to bottom): (1) Position angle PA, (2) ellipticity ϵ, (3-5) Fourier coefficients b_3/a, b_4/a b_6/a. **(b)** Results of the decomposition for the HST data (open symbols - whole galaxy; filled symbols - bulge only) plotted versus the major axis a. Left panels (top to bottom):(1-2) Fourier coefficients a_4/a, a_6/a. Right panels (top to bottom): (1) Position angle PA, (2) ellipticity ϵ.

from the positive a_4 parameter from the isophotal shape analysis (Fig. 4a). Since the disky isophotes extend to the same radius as the counter rotating core, detected in the velocity curves, it is evident that this component is a *central stellar disk*. Additionally, the decomposition of the surface brightness profiles into a central exponential disk profile and a bulge following an $r^{1/4}$ law, yields a perfect remaining bulge with $a_4 = 0$ (Fig. 4b). The central disk in NGC 4816 contributes only 1 % to the total V band light of the galaxy. This is even less than found for the kinematically decoupled central disk inside NGC 5322 (Bender et al. 1994), which has D/G = 3 % (Scorza & Bender 1995). Inside the break radius $r_b = 4$" the central disk of NGC 4816 contributes 6.9 % to the total light. For a thin disk one would expect a positive a_6 parameter from the isophote analysis (Scorza & Bender 1995), but not a negative one as found in our data. Thus, with the assumption of having a thin central disk in NGC 4816 the "measured" inclination is only a lower limit.

The slope of the Mg_b line strength profile steepens inside the break radius r_b (Fig. 2b), which points to a metal enriched core and agrees with results found for other peculiar cores by Bender & Surma (1992). The mean iron index <Fe> and the combined index [MgFe] do also increase inside 8". In the rotation curve the core is only showing up at 4". As it is counter – rotating it has to compete against the superposed rotation of the bulge further out and becomes only dominant inside 4". In fact in (Fig. 2a) you can see that the rotation curve seems to be influenced by the core out to 6" or 7". Comparisons with stellar population models (Worthey 1994) show that the *metallicity* [4] of the core is $Z = \log((Fe/H)/(Fe/H)_\odot) \approx 0.25$ dex *super solar* (Fig. 7a), which is comparable to values measured in central regions of normal galaxies (Faber et al 1995). On the other hand the metallicity of the hosting galaxy drops to values around solar metallicity (outer most data point at $\approx 0.5\ r_e$). In the core as well as in the outer parts of the galaxy the dominating *stellar population is old* (8 – 12 Gyr) (Fig. 7a).

From other studies it is already known that luminous, massive elliptical galaxies can reach a Mg_b to <Fe> overabundance [Mg/Fe] $\approx$ 0.4 dex super solar, while faint early – type galaxies have $\approx$ solar abundances (Gonzales 1993; Fisher et al. 1995). NGC 4816 shows extreme Mg_b to <Fe> *overabundance* of $\approx$ 0.5 dex (Fig. 7b) with no significant abundance difference between the core and its surrounding, which is in agreement with other investigations (Davies et al. 1993; Paquet, 1994). In a recent study, Thomas et al. (1997) show that in addition to a top heavy initial mass function (IMF), a short star formation time scale is needed to explain this light element enrichment in massive elliptical galaxies with an excess of Supernovae II rate.

For **IC 4051** there is evidence for a co-rotating *peculiar core* with a radial size of $r_b = 5$" (Fig. 3a). In contrast to the core NGC 4816 it is not clear whether this central component in IC 4051 is really decoupled. From the presented kinematic data (Fig. 3a), we cannot exclude that IC 4051 is simply a disky elliptical or S0 galaxy being a superposition of a hot (rotating) bulge and a cold, fast rotating disk (Scorza & Bender 1995). In combination with the brightness profiles we derived from the HST images, we can compute the anisotropy parameter (Binney 1978, Kormendy 1982):

$$\left(\frac{v_r}{\sigma_m}\right)^* = \frac{v_r/\sigma_m}{\sqrt{\epsilon/(1-\epsilon)}}, \qquad (1)$$

where v_r is the rotation velocity, ϵ the ellipticity and σ_m the averaged velocity dispersion. Objects with $(v/\sigma)^* > 0.7$ are mainly rotationally flattened, while those having smaller values are flattened by anisotropic velocity dispersions (Davies et al. 1983). Since the anisotropy parameter for IC 4051 is ≈ 0.5 inside the "core" and ≈ 0.4 at r_e it is rather unlikely that it is an S0 galaxy.

From the isophotal analysis and the photometric decomposition (Fig. 5) we inferred that this core is a *central stellar disk*. Like the disk in NGC 4816 it only contributes 0.4 % to the total V band light of the galaxy and 0.5 % to the total I band light. Since the disks in "normal" S0 galaxies contribute $\approx 4 - 11$ % to the total V band light (Scorza & Bender 1995) IC 4051 is probably *not* an S0 galaxy, but contains a decoupled central disk. Inside the break radius $r_b = 5$" the disk of IC 4051 contributes 2.4 % and 2.7 % in the V and I band, respectively. The V-I colour gradient inside the IC 4051's core is shallow and in agreement with Carollo et al. (1997) it does not indicate any significant difference between the core and the surrounding galaxy.

In contrast to NGC 4816 the slope of the Mg_b line profile does not increase inside the core of IC 4051 ($r < 5$") but is constant (Fig. 3b). This lack of steepening inside the core could be due to [NI] emission that can contaminate the Mg absorption feature (Goudfrooij & Emsellem 1996). On the other hand the gradient of the mean iron index <Fe> is enhanced towards the center starting at the break radius, pointing to a *metal enriched* core as found in NGC 4816. Comparisons with stellar population models (Fig. 8a) show that the *metallicity* drops from *super solar* inside the core ($\approx$ 0.25 dex) to -0.5 dex in the outer part of the galaxy (outer most data point at $\approx 1\ r_e$). This metallicity difference of 0.75 dex between the central and the embedding galaxy is unusually high. The stars in the core are *old* (12 –17 Gyr), while an age estimate in the outer parts is not possible since the H_β absorption lines are probably contaminated by emission like features in the outer parts of the galaxy. As in NGC 4816 the dominating stellar population is *highly* [Mg/Fe] *overabundant*.

[4] Following Faber et al. (1995) we used the combined index $[MgFe] = (Mg_b\ <Fe>)^{1/2}$, which represents the mean metallicity best.

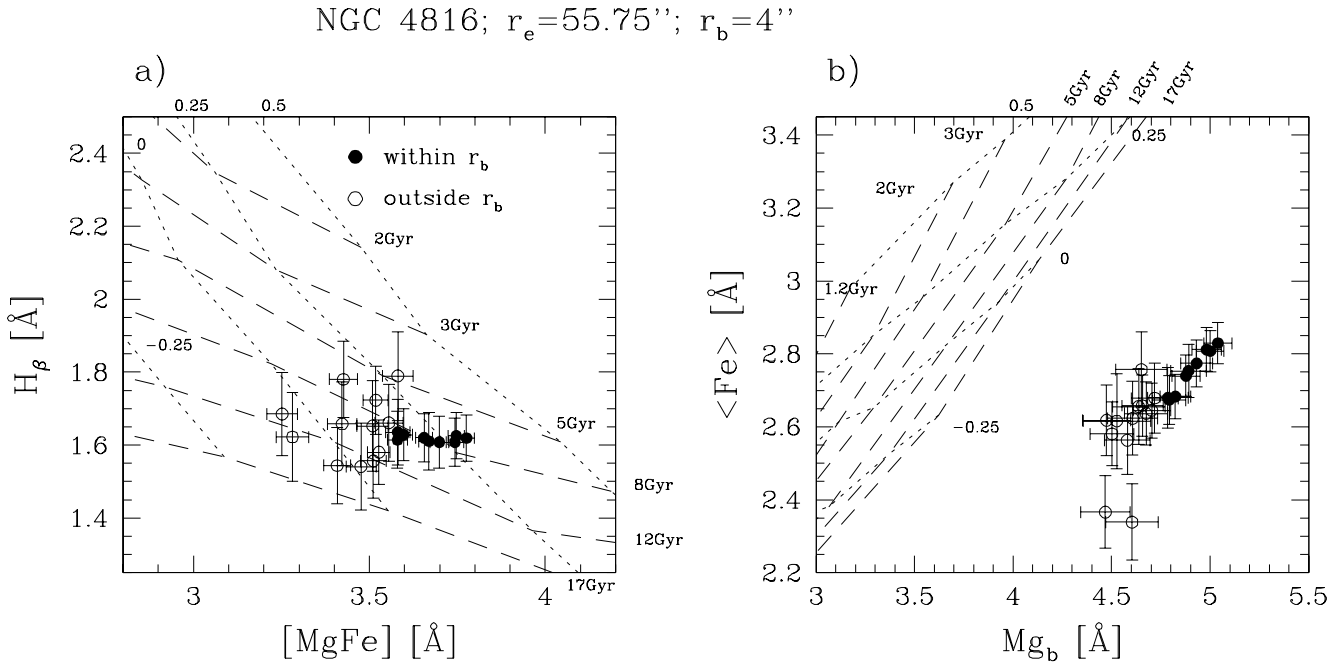

Fig. 7. Measured absorption line indices of NGC 4816 plotted into the model grids of Worthey (1994); dashed lines - constant age in Gyr; dotted lines - constant metallicity $\log(Z/Z_\odot)$. Filled symbols represent measurements inside the break radius r_b, open symbols those for measurements outside r_b. **(a)** The age indicating H_β versus the metallicity indicating combined index [MgFe]. **(b)** <Fe> versus Mg_b index. Obviously the models cannot reproduce the measured element ratios.

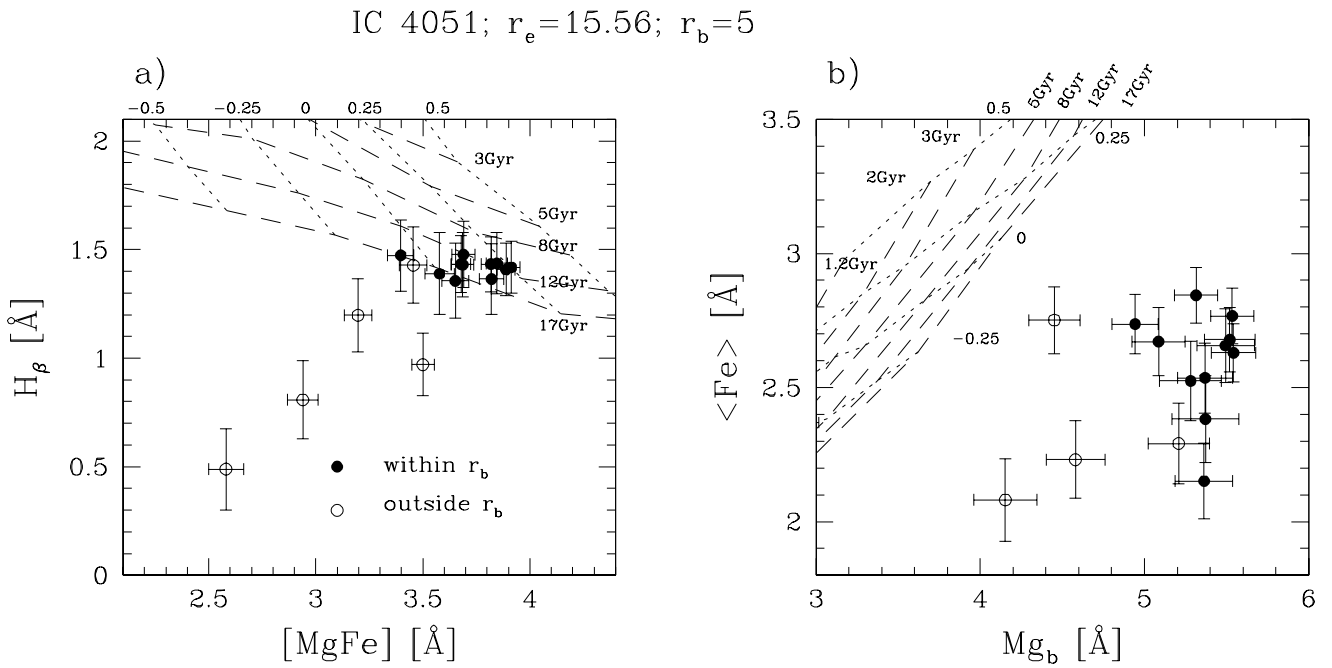

Fig. 8. Measured absorption line indices of IC 4051 plotted into the model grids of Worthey (1994); dashed lines - constant age in Gyr; dotted lines - constant metallicity $\log(Z/Z_\odot)$. Filled symbols represent measurements inside the break radius r_b, open symbols those for measurements outside r_b. **(a)** The age indicating H_β versus the metallicity indicating combined index [MgFe]. Outside r_b the H_β indices are emission contaminated and hence not reliable for age determination. **(b)** <Fe> versus Mg_b index. Obviously the models cannot reproduce the measured element ratios.

5. Discussion

NGC 4816 contains a kinematically decoupled central disk, which is dominated by an old, metals enriched, highly [Mg/Fe] overabundant stellar population and is only contributing ≈ 1 % to the total light of the galaxy. For the formation scenario of this disk we favour *dissipational major merging* for the following reasons:

• A *merging* event is necessary to account for the kinematic decoupling between core and bulge (Barnes 1992b).

• *Dissipational* merging is required in contrast to dissipationless processes because: (1) In a dissipational merger the gas can get to the center and form a *flattened, disk – like* core by dissipation and cooling (Barnes & Hernquist 1996). Flattened systems like the core of NGC 4816 cannot be built through dissipationless processes. (2) While dissipationless merger tend to weaken metallicity gradients (White 1980), only dissipative processes can built up these gradients. Previously enriched gas settles in the core and may trigger the formation of *metal enriched* stars (Bender & Surma 1992) . The enhancement of the stellar metallicity we find in the central disk of NGC 4816 require gas dissipation.

• The accretion of low-mass gas rich galaxies can be ruled out since they are generally too metal poor (Bender & Surma 1992). To obtain the high core metallicity measured in NGC 4816 a *major* merging of massive, star dominated, but gas-rich pro-genitors is needed.

• Finally, merging or interacting galaxies experience a burstlike star formation, that may produce flatter IMFs (Wright et al. 1988; Silk 1992) and hence could help to produce the [Mg/Fe] *overabundance* we measure in the stellar population of NGC 4816.

Since the stellar population of the central disk is likely old, this merging events must have occured at high redshift in the early phase of formation. However, the age indicating H_β line strength is strongly sensitive to H_β emission from younger populations. Hence, the estimated age is only an upper limit to the true age of the stars in the central disk. If the true age was significantly younger, the central disk in NGC 4816 could also have formed in late, gas-rich mergers, which are e.g. observed in ultraluminous IRAS galaxies (Solomon et al. 1992, Prestwich et al. 1994). However, late mergers may have problems in producing the light element overabundances.

The central disk in IC 4051 is also dominated by an old, metal rich, highly [Mg/Fe] overabundant stellar population and contributes only ≈ 1 % to the total light of the galaxy. In contrast to NGC 4816 the interpretation of the data with respect to the formation of the galaxy and its peculiar core is less evident. Whether the disk in IC 4051 is *really* kinematically *decoupled* and hence whether this galaxy is indeed a major merger remnant remains an open question, which can not be answered with our data.

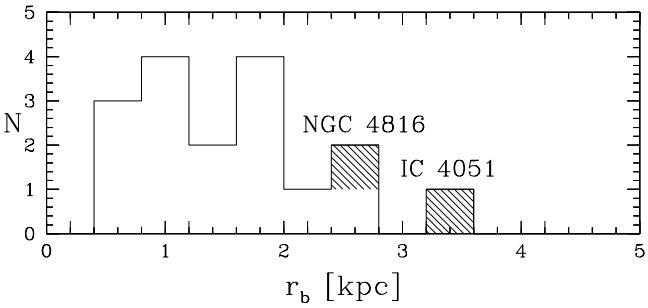

Fig. 9. Distribution of the break radii r_b of all known kinematically distinct cores. The positions of IC 4051 and NGC 4816 are indicated by crosses.

Table 4 contains the 17 known early – type galaxies with clear evidence for a kinematically decoupled core. Most of the other cores have sizes smaller than 2 kpc (see the histogram Fig. 9). With a break radius of $r_b = 2.7$ kpc NGC 4816 hosts one of the largest kinematically decoupled core ever detected in an early – type galaxy. Only the decoupled central of NGC 7626, the dominating galaxy of the Pegasus cluster (Jedrzejewski& Schechter 1988; Balcells & Carter 1993) has a similar size. The peculiar core in IC 4051 ($r_b = 3.4$ kpc) is even bigger. To investigate whether the large cores of NGC 4816 and IC 4051 are systematically different to other, smaller kinematically decouples cores, we compared the properties of their corresponding central disks. HST images are available for 13 of the 15 galaxies that are not in Coma and are listed in Table 4. We applied the D/B decomposition of Scorza & Bender (1995) to derive the properties of the central disks, that are present in 8 of these galaxies. Since 4 of these disks were contaminated with dust we are left with reliable disk properties for NGC 1427, NGC 4365, NGC 5322 and NGC 5982. Plotting the central surface brightness $SB_\circ$ versus the scale length r_h shows that the disks of NGC 4816 and IC 4051 simply represent the "faint", "large" end of a sequence. We therefore speculate that the large cores of NGC 4816 and IC 4051 had formation histories similar to the ones of the smaller, already known decoupled cores. Furthermore, the parameters r_h and $SB_\circ$ derived for the central disks of galaxies with cores are similar to the ones derived for "disky ellipticals" (Scorza & Bender 1995).

Excluding Coma's two dominant galaxies (NGC 4874 & NGC 4889) and the central galaxy (NGC 4839) of the Coma substructure in the S/W (Colless & Dunn 1995), IC 4051 is the third brightest galaxy in the central square degree of the cluster (see Jørgensen & Franx 1994). NGC 4816 is even 0.75 mag brighter than IC 4051 in the R band and hence, both galaxies have luminosities above

Galaxy	vhel (km/s)/ Distance (Mpc)	scaling	r_b	r_e	References
I 4051	7000 / 140	1" = 678 pc	5" = 3.4 kpc	16" = 10.5 kpc	this paper
N 4816	7000 / 140	1" = 678 pc	4"= 2.7 kpc	55.75" = 37.8 kpc	this paper
N 4365*	1153 / 23	1" = 112 pc	8" = 0.9 kpc	64" = 6.4 kpc	BS92, BSG94, B88
N 4406*	1153 / 23	1" = 112 pc	6" = 0.7 kpc	199" = 22.3 kpc	BSG94, BS92, FIH89, B88,
N 4472*	1153 / 23	1" = 112 pc	6" = 0.7 kpc	104" = 11.65 kpc	Setal93, BSG94, DB88
N 4494	1172 / 23	1" = 114 pc	7" = 0.8 kpc	60" = 6.8 kpc	BSG94, BS92, B88, JS88
I 1459	1647 / 33	1" = 160 pc	10" = 1.7 kpc	35" = 5.8 kpc	FI88, FIH89
N 3608	1126 / 23	1" = 109 pc	10" = 1.1 kpc	34" = 3.7 kpc	JS88
N 5322	1963 / 39	1" = 190 pc	10" = 1.9 kpc	34" = 6.5 kpc	BSG94, B88
N 5813	1674 / 33	1" = 162 pc	10" = 1.6 kpc	57" = 9.2 kpc	EEC82
N 7626	3493 / 70	1" = 339 pc	8" = 2.7 kpc	39" = 13.2 kpc	JS88, BC93
N 1427	1411 / 28	1" = 137 pc	8" = 1.1 kpc	33" = 4.5 kpc	D'Oetat95
N 1439	1585 / 32	1" = 154 pc	10" = 1.5 kpc	41" = 6.3 kpc	FIH89
N 1700	4082 / 82	1" = 396 pc	5" = 2.0 kpc	14" = 5.5 kpc	BSG94, FIH89, SSC96
N 5982	2787 / 56	1" = 270 pc	7" = 1.9 kpc	25" = 6.8 kpc	WBM88
N 7796	3252 / 65	1" = 315 pc	4" = 1.3 kpc	27" = 8.5 kpc	Betal94
N 6851	3051 / 61	1" = 296 pc	2.5" = 0.7 kpc	14.5" = 4.3 kpc	TSZ92

Table 4. Galaxies with kinematically decoupled cores mentioned in the literature. We used H_o = 50 km / (s Mpc) to the determine the distances. At the "break radius" r_b the decoupled core starts to dominate the rotation curve. Galaxies with an * belong to the Virgo cluster.

L_*. While NGC 4816 lies 49.0' S/W of the clusters center and only 21.8' apart from NGC 4839, IC 4051 lies only 15.5' N/E of the clusters center. Whereas NGC 4816 is the largest host galaxy (r_e = 37.8 kpc) of a distinct core, the size of IC 4051 is comparable the sizes of the host galaxie listed in Table 4. However, like the other galaxies with kinematically decoupled cores *both* galaxies do not deviate from the Fundamental Plane or the Mg – σ relation. Our total sample of 35 Coma galaxies is complete for galaxies brighter than M_B = -21.6 mag (14 galaxies) and is 1/3 complete in the magnitude range -21.6 mag $< M_B <$ -20.2 mag (21 galaxies). NGC 4816 and IC 4051 both belong to the complete sample. Similarly, in the Virgo cluster there are only two galaxies (NGC 4406 and NGC 4472) that host a decoupled core and are brighter than -21.6 mag. The core of NGC 4406 contributes $\approx$ 20 % to the the V band light inside the kinematically break radius r_b (Surma 1992), which is consistent with the central disks in the Coma galaxies. In the magnitude range -21.6 mag $< M_B <$ -20.2 mag one galaxy with a decoupled core is known in the Virgo cluster (NGC 4365), but none found in the Coma cluster yet. In their detailed discussion of NGC 4365's stellar population and kinematic Surma & Bender (1995) conclude that its core also must have built through dissipational major merging processes. This core also shows disk – like structure, its mean stellar population has a metallicity which is $\approx$ 0.4 dex above the Sun and an age of $\approx$ 7 Gyr. Inside the kinematically break radius r_b it contributes $\approx$ 20 % to the V band light. Note that the break radius r_b of the "Virgo cores" would compare to $<$ 1.3" at Coma's distance. Thus with our observational setups (spatial resolution $\approx$ 1.5") we missed all possibly existing cores with comparable size to the Virgo decoupled cores. On the other hand there is no core detected in the Virgo cluster that has a similar size like those found in the Coma cluster galaxies NGC 4816 and IC 4051. Based on our data, we cannot derive any statistically significant difference between the Coma and the Virgo cluster with respect to the fraction of galaxies with kinematically decoupled/peculiar cores.

Acknowledgements. The authors thank the staff of the Calar Alto and MDM observatory for their effective support. We gratefully acknowledge the helpful discussions with Paola Belloni and Laura Greggio. We also want to thank the referee Marcella Carollo for helpful comments. This work was supported by the Deutsche Forschungsgemeinschaft via project Be 1091/6.

6. References:

Andreon S., Davoust E., Michard R., Nieto J.-L., Poulain P., 1996, A&AS 116, 429
Andreon S., Davoust E., Poulain P., 1997, A&AS 126, 67
Balcells M., 1991, A&A 249, L9
Balcells M., Carter D. 1993, A&A 279, 376 (BC93)
Balcells M., Quinn P.J., 1990, ApJ 361, 381
Barnes J., 1992a, ApJ 393, 484
Barnes J. 1992b, ApJ 471, 115
Barnes J., Hernquist L., 1996, ApJ 471, 115
Bender R., 1988, A&A 202, L5 (B88)
Bender R., 1990, A&A 229, 441
Bender R., Möllenhoff C., 1987, A&A 177, 71

Bender R., Surma P., 1992, A&A 258, 250 (BS92)
Bender R., Saglia R.P., Gerhard O., 1994, MNRAS 269, 785
(BSG94)
Bertin G., Bertola F., Buson L.M., et al., 1994,A&A 292, 381
(Betal94)
Bertola F., Cinzano P., Corsini E.M., Rix H.-W., Zeilinger W.W., 1995, ApJ 448, L13
Binney J., 1978, MNRAS 183, 779
Burstein D., Davies R.L., Dressler A., et al., 1987, ApJS 64,
601
Carollo M., Franx M., Illingworth G.D., Forbes D.A., 1997,
ApJ 481, 710
Colless M., Dunn A., 1996, ApJ 458, 435
Davies R.L., Efstathiou G., Fall S.M., Illingworth G.D., Schechter P.L., 1983, ApJ 266, 41
Davies R.L., Burstein D., Dressler A., et al., 1987, ApJS 64, 581
Davies R.L., Sadler E.M., Peletier R.F., 1993, MNRAS 262,
650
D'Onofrio M., Zaggia S.R., Longo G., Caon N., Capaccioli M.,
1995, A&A 296, 319 (D'Oetal95)
Efstathiou G., Ellis R. S., Carter D., 1982, MNRAS 201, 975
(EEC82)
Faber S.M., Friel E.D., Burstein D., Gaskell C.M., 1985, ApJS 57, 711
Faber S.M., Trager S., Gonzalez J.J., Worthey G., 1995, IAU
Symp. 164 (*Stellar Populations*), ed. P.C. van der Kruit & G. Gilmore, Kluwer Dordrecht
Faber S.M., Tremaine S., Ajhar E., et al., 1997, AJ (in press)
Franx M., Illingworth G.D., 1988, ApJ 327, L55 (FI88)
Franx M. Illingworth G.D., Heckmann T., 1989, ApJ 344, 613
(FIH89)
Fisher D., Franx M., Illingworth G.D., 1995, ApJ 448, 119
Gonzales J.J., 1993, PhD thesis, University of California, Santa Cruz
Goudfrooij P., Emsellem E., 1996, A&A 306, L45
Hernquist L., 1993, ApJ 409, 548
Heyl J.S., Hernquist L., Spergel D.N., 1994, ApJ 427, 165
Holtzman J.A., Burrows C.J., Casertano S., et al. 1995 PASP 107, 1065
Jaffe W., Ford H.C., O'Connell R.W., van den Bosch F.C., Ferrarese L., 1994, AJ 108, 1567
Jedrzejewski R., Schechter P.L., 1988, ApJ 330, L87 (JS88)
Jørgensen I., Franx M., 1994, ApJ 433, 553
Jørgensen I., Franx M., Kjærgaard P., 1992, A&AS 95, 489
Jørgensen I., Franx M., Kjærgaard P., 1995, MNRAS 276, 1341
Kormendy J., 1982, in *Morphology and Dynamics of Galaxies*,
eds. Martinet, L., Mayor, M., Saas Fee
Kormendy J., 1984, ApJ 287, 577
Kormendy J., Sanders D.B., 1992, ApJ 390, L53
Lauer T.R., Ajhar E.A., Byun Y.-I., et al., 1995, AJ 110, 2622
Lucey J.R., Guzmán R., Carter D., Terlevich R.J., 1991, MNRAS 253, 584
Mehlert D., 1998, PhD thesis, Universität München
Nieto J.-L., Bender R., Arnaud J., Surma P., 1991, A&A 244, L25
Paquet A., 1994, PhD thesis, University of Heidelberg
Poulain P., Nieto J.-L., 1994, A&AS 103, 573
Prestwich A.H., Joseph R.D., Wright G.S., 1994, ApJ 422, 72
Rix H.-W., White S.D.M., 1992, MNRAS 254, 389
Rocca-Volmerange B., Guiderdoni B., 1988, A&AS 75, 93
Saglia R.P., Bertin G., Bertola F., et al., 1993, ApJ 403, 567
(Setal93)
Saglia R.P., Bertschinger G., Baggley G., et al., 1997a, ApJS 109, 79
Saglia R.P., Burstein D., Bertschinger G., etal., 1997b, MNRAS (in press; Setal97b)
Schweizer F., 1990, in 'Dynamics and Interactions of Galaxies', ed. R. Wielen, Springer – Verlag, p.60
Scorza C., Bender R., 1995, A&A 293, 20
Seaton M.J., 1979, MNRAS 187, 785
Silk J., 1992, , IAU Symp. 149 (*The Stellar Populations of*
Galaxies), ed. B. Barbuy, Kluwer Dordrecht
Solomon P.M., Downes D., Radford S.J.E., 1992, ApJ 387, L55
Statler T.S., Smecker-Hane T., Cecil, G.N, 1996, AJ 111,1512
(SSC96)
Surma P., 1992, PhD thesis, Universität Heidelberg
Surma P., Bender R., 1995, A&A 298, 405
Thomas D., Greggio L., Bender R., 1997, MNRAS (in press)
Tody D., 1993, Astronomical Data Analysis Software and Systems II, A.S.P. Conference Series 52, eds. R.J. Hanisch,
R.J.V. Brissenden, J. Barnes
Toniazzo T., Stiavelli M., Zeilinger W.W., 1992, A&A 259, 39
(TSZ92)
van der Marel R.P., Franx M., 1993, ApJ 407, 525
Wagner S.J., Bender R., Möllenhoff C., 1988, A&A 195, L5
(WBM88)
White S.D.M., 1980, MNRAS 191, 1

Worthey G., 1992, PhD thesis, University of California, Lick
Observatory
Worthey G., 1994, ApJS 95, 105
Wright G.S., Joseph R.D., Robertson N.A., James P.A., Meikle W.P.S, 1988, MNRAS 233, 1

This article was processed by the author using Springer-Verlag LaTeX A&A style file *L-AA* version 3.